


 Cite this: *Chem. Commun.*, 2024, 60, 885

 Received 21st November 2023,
 Accepted 14th December 2023

DOI: 10.1039/d3cc05709g

rsc.li/chemcomm

Selective dehydrogenation of ammonia borane to polycondensated BN rings catalysed by ruthenium olefin complexes†

 Daniel Himmelbauer,^{‡,ab} Fabian Müller,^{‡,a} Clara Schweinzer,^{ib,a} Fernando Casas,^a Bruno Pribanic,^a Grégoire Le Corre,^{ib,a} Debora Thöny,^{ib,a} Monica Trincado^{ib,*a} and Hansjörg Grützmacher^{ib,*a}

Dehydrogenation of ammonia borane to well-defined products is an important but challenging reaction. A dinuclear ruthenium complex with a Ru–Ru bond bearing a diazadiene (dad) unit and olefins as non-innocent ligands catalyzes the highly selective formation of conjugated polycondensed borazine oligomers (B_xN_xH_y), predominantly B₂₁N₂₁H₁₈, the BN analogue of superbenzene.

Ammonia borane, H₃N–BH₃ (AB) is an interesting chemical hydrogen carrier (19.6 wt% of hydrogen) and its dehydrogenation has been intensively investigated during the past few years.¹ To avoid the rather harsh and unselective conditions of thermal decomposition,² homogeneously metal-catalysed dehydrogenations using Sc,³ Y,⁴ Ti,⁵ Cr,⁶ Mo,^{6,7} W,⁶ Re,⁸ Fe,⁹ Ru,¹⁰ Os,¹¹ Co,¹² Rh,¹³ Ir,^{7b,10a,14} Ni,¹⁵ Pd,¹⁶ Th and U¹⁷ complexes have been studied, under aprotic conditions. Transition metal complexes are also well-established catalysts for the highly efficient hydrolysis of AB, frequently operating at ambient temperature.¹⁸ These reactions give hydrogen (as chemical energy carrier), but also ammonia – a poison for proton exchange membrane (PEM) fuel cells – and the formation of multiple borate products, whose reduction to regenerate the spent fuel is thermodynamically highly challenging. Numerous catalysts with main group element centres as active sites and organocatalysts also dehydrogenate AB, albeit with lesser efficacy.¹⁹ Up to 2.7 equivalents of hydrogen can be released by the most efficient Ru catalyst at 1 mol% loading (Fig. 1) in aprotic media.^{10g,20} Most catalysts that dehydrogenate ammonia borane lead to the formation of insoluble poly(aminoborane) (NH₂BH₂)_n,^{7b,9a,c,10b,e,11,14} or a mixture

of borazine and polycondensated borazines as reaction products.^{9a,10f,15,16,19a} The selectivity of these transformations depends on whether aminoborane (H₂B=NH₂), a highly reactive intermediate formed in the first dehydrogenation step, remains coordinated to the metal centre or not. The “on-metal” reaction path leads to poly(aminoboranes) *via* a chain-growth mechanism reminiscent of ethylene polymerisation. In the “off-metal” reaction path, H₂B=NH₂ is released to give oligomers (H₂NBH₂)_n, which upon further dehydrogenation might afford borazine, B₃N₃H₃, and polycondensed borazine molecules (B_xN_xH_x) (x < n).²¹ Both compounds, as well as other AB oligomers are suitable precursors for the generation of thin layers of *h*-BN (hexagonal boron nitrides).²² These have a wide range of applications, for example, as UV light emitters,²³ components of polymer nanocomposite membranes for hydrogen separation²⁴ or as precursors to BCN materials.²⁵ To the best of our knowledge, the synthesis of well-defined BN sheets by catalysed dehydrogenation of ammonia borane has not been reported so far.

Here, we report a dinuclear Ru olefin complex as active and selective catalyst for the dehydrogenation of ammonia borane (Fig. 1). The catalyst forms selectively extended but well-defined polycondensed borazine rings (B_xN_xH_y), predominantly BN-hexabenzocoronene B₂₁N₂₁H₁₈ (**BN21**).

The diruthenium complex **2** was prepared by hydrolysis of the previously reported ruthenium hydride **1**^{26a} in THF at 70 °C

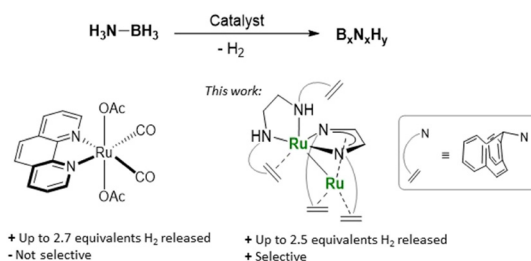


Fig. 1 Selected state-of-the-art catalyst for the dehydrogenation of H₃N–BH₃ (**AB**) and new Ru catalyst.

^a Department of Chemistry and Applied Biosciences, ETH Zurich Vladimir-Prelog-Weg 1, Zurich CH-8049, Switzerland. E-mail: trincado@inorg.chem.ethz.ch, hgruetzmacher@ethz.ch

^b Institute of Applied Synthetic Chemistry, TU Wien, Getreidemarkt 9/163, Vienna A-1060, Austria

† Electronic supplementary information (ESI) available. CCDC 2108631. For ESI and crystallographic data in CIF or other electronic format see DOI: <https://doi.org/10.1039/d3cc05709g>

‡ These authors contributed equally.



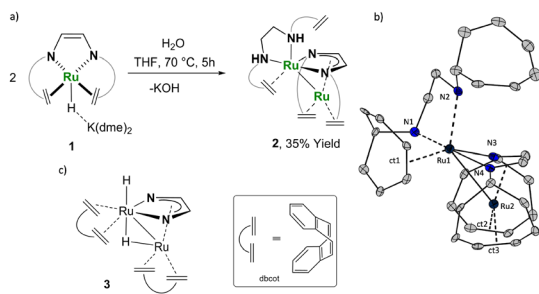


Fig. 2 (a) Synthesis of complex **2**. (b) ORTEP drawing of the molecular structure of **2**. Non-relevant hydrogen atoms, trop-benzo rings, and solvent molecules are omitted for clarity. Selected bond lengths (Å) and angles ($^\circ$): Ru1–Ru2 2.7119(6), Ru1–N2 2.252(2), Ru1–N1 2.142(2), Ru1–N3 2.119(2), Ru1–N4 2.157(2), Ru2–N3 2.095(2), Ru2–N4 2.086(2), N1–C31 1.488(4), N2–C32 1.499(4), C31–C32 1.510(4), C19–C20 1.344(4), C36–C37 1.452(4), N1–Ru1–N2 79.3(1), N3–Ru2–N4 77.9(1). (c) Drawing of complex **3** $[\text{Ru}_2(\mu\text{-H})(\text{Me}_2\text{dad})(\text{dbcot})_2]$.

in a closed reaction vessel (Fig. 2a). Crystals suitable for X-ray diffraction analysis were obtained directly from the reaction mixture by slow cooling to room temperature.

Complex **2** contains a dinuclear ruthenium core which is non-symmetrically bridged by a 1,4-bis[5*H*-dibenzo[*a,d*]cyclohepten-5-yl]-1,4-diazabuta-1,3-diene (trop_2dad) ligand (Fig. 2b). As such, **2** has a similar structure to the recently published dinuclear Ru complex $[\text{Ru}_2\text{H}(\mu\text{-H})(\text{Me}_2\text{dad})(\text{dbcot})_2]$ **3** (Me_2dad = *N,N'*-dimethyl-1,4-diazadiene, dbcot = dibenzo[*a,e*]cyclooctatetraene; see Fig. 2c)^{26b} and the related Ru carbonyl diazadiene complexes $[\text{Ru}_2(\text{CO})_5(\text{R}_2\text{dad})]$.²⁷ As in these complexes, the structure of **2** is best described with a folded ruthenadiazacyclopentadienide that undergoes η^5 -coordination to a second ruthenium centre (Ru2). This central five-membered ring is formed from Ru1 and a $\text{trop}_2\text{dad}^{2-}$ enediamido ligand. The assignment of the electronic configuration of the ligand is based on the relatively long $\text{N}-\text{C}_{\text{avg}}$ = 1.389 Å and comparatively short $\text{C}=\text{C}$ = 1.377 Å bond distances, which indicate a reduced form of a diazadiene ligand. Formally, this results in an oxidation state of +2 for Ru1 and consequently a zerovalent Ru2. The coordination sphere of Ru2 is completed by two olefinic $\text{C}=\text{C}_{\text{trop}}$ units from two trop units pending from the nitrogen centres of the RuN_2C_2 ring (indicated by the centroids ct2 and ct3 in Fig. 2b). Apart from the $\kappa^2\text{-N,N'}$ coordination to one trop_2dad ligand, the coordination sphere of Ru1 is completed by $\kappa^2\text{-N,N'}$ and $\text{C}=\text{C}_{\text{trop}}$ coordination of a trop_2dae ligand (dae = diaminoethane), of which one $\text{C}=\text{C}_{\text{trop}}$ unit remains uncoordinated. The short Ru–Ru distance (2.714 Å) indicates a direct bond (and would support the formulation of complex **2** with two d^7 -valence configured Ru(I) centres).²⁸ It is presently not possible to assign with certainty oxidation states to Ru1 or Ru2.²⁹ The relatively long bond distances of the coordinated olefinic $\text{C}=\text{C}_{\text{trop}}$ units [1.448(6) Å–1.450(6) Å] and significantly low frequency ^{13}C chemical shifts assigned to the olefinic carbons [$\delta(^{13}\text{C})$ 44.5–69.9 ppm; compare to values > 120 ppm for uncoordinated trop_2dad derivatives³⁰] indicate a substantial π -electron back donation from the metal centres into the antibonding $\pi^*(\text{C}=\text{C})$ -orbitals.³¹

Ammonia borane (AB) (2.2 M solution in THF) was catalytically dehydrogenated using 3 mol% of **1** or **2** in THF at 70°C

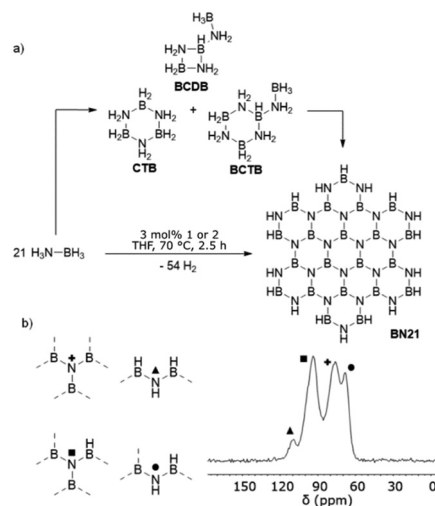


Fig. 3 (a) Synthesis of BN nanosheet **BN21**, showing the intermediates CTB, BCDB and BCTB, as observed by ^{11}B NMR analysis. (b) ^{15}B MAS NMR spectrum of **BN21** and assignment of the resonances based on quantum chemical calculations.^{33,35}

forming soluble polyborazine within 2.5 h (Fig. 3a). If the mononuclear ruthenium hydride **1** is used as a catalyst, it needs to be added to the reaction mixture in three subsequent separated batches. After each addition of **1** (1 mol%), hydrogen evolution is observed immediately (without induction period) but then the activity starts to decrease (see Fig. S6, ESI†). Once catalyst **1** is added, the initial red solution changes rapidly to purple, then subsequently to yellow and brown, which in combination with the loss of activity indicates catalyst deactivation. Attempts to analyse the reaction mixture after catalytic activity ceased failed. Note that if the total amount of catalyst (3 mol%) is added at once at the beginning of the reaction, no clear solution is obtained but a white precipitate appears due to the formation of polyaminoboranes, $(\text{BH}_2\text{NH}_2)_n$. In contrast, the dinuclear complex **2** does not suffer from deactivation and can be loaded in one batch. Complex **2** is sparingly soluble in THF but readily dissolves in the presence of AB. The catalysis proceeds in homogeneous solution: The addition of mercury has no impact on the conversion rate. But addition of triphenylphosphine in excess and sub-stoichiometric amounts (with respect to catalyst concentration) leads to complete or partial loss of activity, respectively. These experiments exclude metal nanoparticles as active species and indicate that soluble complexes with free-coordination sites are responsible for the catalytic activity. The dehydrogenation reaction with the mono-nuclear ruthenium complex **1** was followed by ^{11}B -NMR spectroscopy (Fig. S7, ESI†). After the addition of the 1st mol% of catalyst and heating for 1 h at 70°C , several intermediates were detected, such as cyclotriborazane (CTB) and its constitutional isomer, *B*-(cyclodiborazanyl)amine-borane (BCDB) with a four-membered B_2N_2 ring (Fig. 3a). Both are trimers of aminoborane ($\text{H}_2\text{N}=\text{BH}_2$). Furthermore, the tetramer *B*-(cyclotriborazanyl)amine-borane (BCTB) with a six-membered B_3N_3 ring to which an NH_2-BH_3 group is attached was detected (Fig. 3a).^{21a,32} The same intermediates were detected in reactions with complex **2**. After the second addition of catalyst **1** (1 mol%) and heating for an additional hour, the concentration of



these intermediates significantly decreased, while the one assigned to the polyborazine product increased. After addition of the last 1 mol% of **1** and heating for an additional 1 h, all intermediates were converted. Only two broad ^{11}B NMR signals were detected in solution characteristic for polyborazylene-type structures.³³ The signal of higher intensity at $\delta(^{11}\text{B}) = 29$ ppm indicates of tertiary boron nuclei in a trigonal planar coordination sphere bound to three nitrogen centres (BN_3). The signal at $\delta(^{11}\text{B}) = 32$ ppm is lower in intensity and is assigned to secondary $(\text{BH})\text{N}_2$ units, in agreement with reported literature.^{10g,34}

The ruthenium complexes **1** or **2** do not react with borazine, $\text{B}_3\text{N}_3\text{H}_6$. The catalytic dehydrogenative coupling of the diammoniate of diborane $[\text{H}_2\text{B}(\text{NH}_3)_2]^+[\text{BH}_4]^-$ (**DADB**) by complex **1** or **2** yielded only insoluble polyaminoborane (Fig. S8, ESI †). The soluble BN product was isolated by filtration over Florisil $^\text{®}$ followed by solvent evaporation and analysis by MALDI-TOF mass spectrometry and NMR spectroscopy. Observation of a main signal at 540 m/z and isotope distribution in the mass spectrum indicates that the main product of the catalytic reaction is $\text{B}_{21}\text{N}_{21}\text{H}_{18}$ (**BN21**) (Fig. 3a). Smaller signals were observed for molecular formulas of $\text{B}_{27}\text{N}_{27}\text{H}_{21}$, $\text{B}_{31-36}\text{N}_{31-36}\text{H}_{22-23}$, $\text{B}_{43}\text{N}_{43}\text{H}_{30}$ and $\text{B}_{48-50}\text{N}_{49}\text{H}_{28}$ (see Fig. S10–S15 in ESI † for details). To gain more structural information, ^{15}N -MAS solid state NMR spectra were recorded of the dehydrogenated material formed from the ^{15}N -labelled AB, revealing four signals of different intensities (Fig. 3b). The D_{3h} symmetric structure shown in Fig. 3a for this $\text{B}_{21}\text{N}_{21}\text{H}_{18}$ isomer was predicted by Gastreich *et al.* using DFT methods and will exhibit four ^{15}N resonances in a 1:2:2:2 ratio (see Fig. S9 and Table S2, ESI †).³³ The relative intensity and experimentally observed chemical shifts are in good agreement with the proposed BN polycyclic structure of **BN21** – an BN analogue of “superbenzene” or hexabenzocoronene³⁵ – with an estimated diameter of 11.4 Å.³⁶ We cannot exclude other structures such as those for the teranthene isomer but the corresponding BN analogue has lower symmetry (C_{2v}) and more signals would be expected in the ^{15}N -NMR spectrum (see ESI † for details). Furthermore, dynamic light scattering experiments (DLS) were performed. The observed size distribution (Fig. S16, ESI †) is consistent with the expected average nanosheet length of **BN21**.^{37,38} For the formation of **BN21**, 21 ammonia borane molecules have been coupled leading to the release of 54 molecules of hydrogen. This corresponds theoretically to the evolution of 2.57 equivalents of hydrogen, which is in good agreement with the experimentally measured amount (183.0 mL, 2.52 equiv., TON = 84). On the contrary, the dehydrogenative coupling reaction of AB catalysed by the related dinuclear ruthenium complex $[\text{Ru}_2(\mu\text{-H})(\text{H})(\text{Me}_2\text{dad})(\text{dbcot}_2)]$ (**3**) (Fig. 1c) only produced one equivalent of hydrogen and insoluble polyaminoborane as only product (Fig. S18, ESI †).

In summary, the ruthenium complexes (**1** or **2**) are selective catalysts for the dehydrogenation of ammonia borane to polycondensed borazines compounds of nanometer size such as **BN21**. It is likely, that this “superbenzene” BN analogue has also been formed as soluble polycondensed borazine in previously investigated reactions, but was never characterized as such. In accord with previous studies, we assume that the first dehydrogenation step of AB leads to amino borane, $\text{H}_2\text{N}=\text{BH}_2$ as highly

reactive intermediate, which is released into solution forming cyclic oligomers (**CTB**, **BCDB**, and **BCTB**). These were detected as intermediates in reactions with the mononuclear Ru complex **1** or dinuclear complex **2**. Although no further details on possible reaction mechanism can be given at this time and remains unclear whether mononuclear or polynuclear complexes are responsible for the formation of “superbenzene” type BN compounds, we are confident that our findings will help to find better catalysts to prepare and isolate these fascinating and potentially useful BN nanosheets in high yield.

We thank Jonas Bösken for the synthesis of complex **3**. We also would like to acknowledge Bill Ewing, from BoronSpecialities LLC, for fruitful discussions and generous donation of BN substrates. This research was funded by the Austria Science Fund (FWF) (J-4571-N), SNF (grants 192106, 181966) and ETH-Zürich.

Conflicts of interest

There are no conflicts to declare

Notes and references

- (a) M. G. Hu, R. A. Geanangel and W. W. Wendlandt, *Thermochim. Acta*, 1978, **23**, 249–255; (b) B. J. Coe and S. J. Glenwright, *Coord. Chem. Rev.*, 2000, **203**, 5–80.
- (a) V. Sit, R. A. Geanangel and W. W. Wendlandt, *Thermochim. Acta*, 1987, **113**, 379–382; (b) G. Wolf, J. Baumann, F. Baitalow and F. P. Hoffmann, *Thermochim. Acta*, 2000, **343**, 19–25; (c) F. Baitalow, J. Baumann, G. Wolf, K. Jaenicke-Rößler and G. Leitner, *Thermochim. Acta*, 2002, **391**, 159–168.
- P. Xu and X. Xu, *Organometallics*, 2019, **38**, 3212–3217.
- E. Lu, Y. Yuan, Y. Chen and W. Xia, *ACS Catal.*, 2013, **3**, 521–524.
- (a) T. J. Clark, C. A. Russell and I. Manners, *J. Am. Chem. Soc.*, 2006, **128**, 9582–9583; (b) D. Pun, E. Lobkovsky and P. J. Chirik, *Chem. Commun.*, 2007, 3297–3299.
- Y. Kawano, M. Uruichi, M. Shimoi, S. Taki, T. Kawaguchi, T. Kakizawa and H. Ogino, *J. Am. Chem. Soc.*, 2009, **131**, 14946–14957.
- (a) J. A. Buss, G. A. Edouard, C. Cheng, J. Shi and T. Agapie, *J. Am. Chem. Soc.*, 2014, **136**, 11272–11275; (b) A. Staubitz, A. Presa Soto and I. Manners, *Angew. Chem., Int. Ed.*, 2008, **47**, 6212–6215.
- (a) Y. Jiang and H. Berke, *Chem. Commun.*, 2007, 3571–3573; (b) V. Yempally, S. Moncho, Y. Wang, S. J. Kyran, W. Y. Fan, E. N. Brothers, D. J. Darensbourg and A. A. Bengali, *Organometallics*, 2019, **38**, 2602–2609.
- (a) R. T. Baker, J. C. Gordon, C. W. Hamilton, N. J. Henson, P.-H. Lin, S. Maguire, M. Murugesu, B. L. Scott and N. C. Smythe, *J. Am. Chem. Soc.*, 2012, **134**, 5598–5609; (b) C. Lichtenberg, M. Adelhardt, T. L. Gianetti, K. Meyer, B. de Bruin and H. Grützmaier, *ACS Catal.*, 2015, **5**, 6230–6240; (c) N. T. Coles, M. F. Mahon and R. L. Webster, *Organometallics*, 2017, **36**, 2262–2268; (d) J. R. Vance, A. P. M. Robertson, K. Lee and I. Manners, *Chem. – Eur. J.*, 2011, **17**, 4099–4103.
- (a) A. Friedrich, M. Drees and S. Schneider, *Chem. – Eur. J.*, 2009, **15**, 10339–10342; (b) B. L. Conley and T. J. Williams, *Chem. Commun.*, 2010, **46**, 4815–4817; (c) A. Staubitz, M. E. Sloan, A. P. M. Robertson, A. Friedrich, S. Schneider, P. J. Gates, J. Schmedt auf der Günne and I. Manners, *J. Am. Chem. Soc.*, 2010, **132**, 13332–13345; (d) B. L. Conley, D. Guess and T. J. Williams, *J. Am. Chem. Soc.*, 2011, **133**, 14212–14215; (e) X. Zhang, L. Kam and T. J. Williams, *Dalton Trans.*, 2016, **45**, 7672–7677; (f) Z. Lu, B. L. Conley and T. J. Williams, *Organometallics*, 2012, **31**, 6705–6714; (g) X. Zhang, Z. Lu, L. K. Foellmer and T. J. Williams, *Organometallics*, 2015, **34**, 3732–3738; (h) X. Zhang, L. Kam, R. Trerise and T. J. Williams, *Acc. Chem. Res.*, 2017, **50**, 86–95.
- M. A. Esteruelas, A. M. López, M. Mora and E. Oñate, *ACS Catal.*, 2015, **5**, 187–191.
- S. Todisco, L. Luconi, G. Giambastiani, A. Rossin, M. Peruzzini, I. E. Golub, O. A. Filippov, N. V. Belkova and E. S. Shubina, *Inorg. Chem.*, 2017, **56**, 4296–4307.



- 13 (a) C. A. Jaska, K. Temple, A. J. Lough and I. Manners, *J. Am. Chem. Soc.*, 2003, **125**, 9424–9434; (b) C. A. Jaska, K. Temple, A. J. Lough and I. Manners, *Chem. Commun.*, 2001, 962–963; (c) C. A. Jaska and I. Manners, *J. Am. Chem. Soc.*, 2004, **126**, 2698–2699; (d) C. A. Jaska and I. Manners, *J. Am. Chem. Soc.*, 2004, **126**, 1334–1335; (e) C. A. Jaska and I. Manners, *J. Am. Chem. Soc.*, 2004, **126**, 9776–9785; (f) Y. Chen, J. L. Fulton, J. C. Linehan and T. Autrey, *J. Am. Chem. Soc.*, 2004, **127**, 3254–3255; (g) G. M. Adams, D. E. Ryan, N. A. Beattie, A. I. McKay, G. C. Lloyd-Jones and A. S. Weller, *ACS Catal.*, 2019, **9**, 3657–3666; (h) S. Pal, S. Kusumoto and K. Nozaki, *Organometallics*, 2018, **37**, 906–914; (i) G. M. Adams, A. L. Colebatch, J. T. Skornia, A. I. McKay, H. C. Johnson, G. C. Lloyd-Jones, S. A. Macgregor, N. A. Beattie and A. S. Weller, *J. Am. Chem. Soc.*, 2018, **140**, 1481–1495.
- 14 M. C. Denney, V. Pons, T. J. Hebden, D. M. Heinekey and K. I. Goldberg, *J. Am. Chem. Soc.*, 2006, **128**, 12048–12049.
- 15 R. J. Keaton, J. M. Blacquiére and R. T. Baker, *J. Am. Chem. Soc.*, 2007, **129**, 1844–1845.
- 16 S. K. Kim, W. S. Han, T. J. Kim, T.-Y. Kim, S. W. Nam, M. Mitoraj, Ł. Piekos, A. Michalak, S. J. Hwang and S. O. Kang, *J. Am. Chem. Soc.*, 2010, **132**, 9954–9955.
- 17 K. A. Erickson and J. L. Kiplinger, *ACS Catal.*, 2017, **7**, 4276–4280.
- 18 For a review, see: H. L. Jiang and Q. Xu, *Catal. Today*, 2011, **170**, 56–63.
- 19 For selected examples, see: (a) M. Hasenbeck, J. Becker and U. Gellrich, *Angew. Chem., Int. Ed.*, 2020, **59**, 1590–1594; (b) Z. Mo, A. Rit, J. Campos, E. L. Kolychev and S. Aldridge, *J. Am. Chem. Soc.*, 2016, **138**, 3306–3309; (c) D. H. A. Boom, A. R. Jupp and J. C. Slootweg, *Chem. – Eur. J.*, 2019, **25**, 9133–9152.
- 20 (a) D. Han, F. Anke, M. Trose and T. Beweries, *Coord. Chem. Rev.*, 2019, **380**, 260–286; (b) A. Rossin and M. Peruzzini, *Chem. Rev.*, 2016, **116**, 8848–8872.
- 21 (a) H. A. Kalviri, F. Gärtner, G. Ye, I. Korobkov and R. T. Baker, *Chem. Sci.*, 2015, **6**, 618–624; (b) S. Bhunya, P. M. Zimmerman and A. Paul, *ACS Catal.*, 2015, **5**, 3478–3493.
- 22 (a) G. R. Whittell and I. Manners, *Angew. Chem., Int. Ed.*, 2011, **50**, 10288–10289; (b) X. Wang, T. N. Hooper, A. Kumar, I. K. Priest, Y. Sheng, T. O. M. Samuels, S. Wang, A. W. Robertson, M. Pacios, H. Bhaskaran, A. S. Weller and J. H. Warner, *CrystEngComm*, 2017, **19**, 285–294.
- 23 Y. Kubota, K. Watanabe, O. Tsuda and T. Taniguchi, *Science*, 2007, **317**, 932–934.
- 24 Y. Wang, Z.-X. Low, S. Kim, H. Zhang, X. Chen, J. Hou, J. G. Seong, Y. M. Lee, G. P. Simon, C. H. J. Davies and H. Wang, *Angew. Chem., Int. Ed.*, 2018, **57**, 16056–16061.
- 25 D. Marinelli, F. Fasano, B. Najjari, N. Demitri and D. Bonifazi, *J. Am. Chem. Soc.*, 2017, **139**, 5503–5519.
- 26 (a) R. E. Rodriguez-Lugo, M. Trincado, M. Vogt, F. Tewes, G. Santiso-Quinones and H. Grützmacher, *Nat. Chem.*, 2013, **5**, 342–347; (b) X. Yang, T. L. Gianetti, M. D. Wörle, N. P. van Leest, B. de Bruin and H. Grützmacher, *Chem. Sci.*, 2019, **10**, 1117–1125.
- 27 (a) K. Vrieze, *J. Organomet. Chem.*, 1986, **300**, 307–326; (b) D. Brazzolotto, M. Gennari, N. Queyriaux, T. R. Simmons, J. Pécaut, S. Demeshko, F. Meyer, M. Orio, V. Artero and C. Duboc, *Nat. Chem.*, 2016, **8**, 1054–1060.
- 28 The intermetallic distance is similar to values reported for a Ru–Ru single bond in related structures containing a phenylene diamido coordinated to a Ru(II) dimer: A. Anillo, M. R. Diaz, S. Garcia-Granda, R. Obeso-Rosete, A. Galindo, A. Ienco and C. Mealli, *Organometallics*, 2004, **23**, 471.
- 29 (a) F. Hartl, M. P. Aarnts, H. A. Nieuwenhuis and J. van Slageren, *Coord. Chem. Rev.*, 2002, **230**, 107–125; (b) F. J. de Zwart, B. Reus, A. A. H. Laporte, V. Sinha and B. de Bruin, *Inorg. Chem.*, 2021, **60**(5), 3274–3281.
- 30 C. Böhler, “Synthesis of new types of trop ligands to stabilize low-valent metal centers” *ETH dissertation*, No. 144420, 2001.
- 31 V. Sinha, B. Pribanic, B. de Bruin, M. Trincado and H. Grützmacher, *Chem. – Eur. J.*, 2018, **24**, 5513–5521.
- 32 A. Staubitz, A. P. M. Robertson and I. Manners, *Chem. Rev.*, 2010, **110**, 4079–4124.
- 33 M. Gastreich, *Werkzeuge zur Modellierung von Siliciumbornitrid-Keramiken: Entwicklung von Mehrkörperpotenzialen und Berechnung zur NMR-chemischen Verschiebung*. PhD diss., Bonn, 2001.
- 34 For ¹¹B solid-state NMR data of both boron sites in polyborazylene, see: J. Li, S. Bernard, V. Salles, C. Gervais and P. Miele, *Chem. Mater.*, 2010, **22**, 2010–2019.
- 35 (a) J. Wu, M. D. Watson, N. Tchegotareva, Z. Wang and K. Müllen, *J. Org. Chem.*, 2004, **69**, 8194–8204; (b) S. Ito, P. T. Herwig, T. Böhme, J. P. Rabe, W. Rettig and K. Müllen, *J. Am. Chem. Soc.*, 2000, **122**, 7698–7706.
- 36 R. Boese, A. H. Maulitz and P. Stellberg, *Chem. Ber.*, 1994, **127**, 1887–1889.
- 37 H. P. Ederle and H. Nöth, *Eur. J. Inorg. Chem.*, 2009, 3398–3402.
- 38 M. Lotya, A. Rakovich, J. F. Donegan and J. N. Coleman, *Nanotechnology*, 2013, **24**, 265703.

